CHINESE OPTICS LETTERS

Vol. 21, No. 1 | January 2023

Single-layered non-interleaved spin-insensitive metasurfaces for wavefront engineering

Ata Ur Rahman Khalid[1], Naeem Ullah[2], Yu Han (韩 遇)[3], Urooj Asghar[4], Xiaocong Yuan (袁小聪)[1*], and Fu Feng (冯 甫)[1**]

[1] Nanophotonics Research Center, Shenzhen Key Laboratory of Micro-Scale Optical Information Technology & Institute of Microscale Optoelectronics, Shenzhen University, Shenzhen 518000, China

[2] College of Physics and Optoelectronics Engineering, Shenzhen University, Shenzhen 518000, China

[3] Beijing Engineering Research Center for Mixed Reality and Advanced Display, School of Optics and Photonics, Beijing Institute of Technology, Beijing 100081, China

[4] Department of Physics, Forman Christian College-University, Lahore 54600, Pakistan

*Corresponding author: xcy@szu.edu.cn

**Corresponding author: fufeng@szu.edu.cn

Received September 16, 2022 | Accepted November 11, 2022 | Posted Online January 17, 2023

Metasurfaces, two-dimensional (2D) or quasi-2D arrays of dielectric or metallic meta-atoms, offer a compact and novel platform to manipulate the amplitude, phase, and polarization of incoming wavefronts in a desired manner by engineering the geometry of meta-atoms. In polarization control, spin-insensitive metasurfaces have attracted significant attention due to the robustness of circular polarization against the beam misalignment and multi-path effects. Till now, several efforts have been made to realize polarization-insensitive metasurfaces for circularly polarized (CP) wavefront manipulation; however, these metasurfaces only consider the cross-polarization channels and keep the co-polarization channels abandoned. Such metasurfaces cannot be considered truly spin-insensitive, as one has to carefully choose the analyzer at output. Here, by combining the polarization-insensitive geometric phase and engineered propagation phase, we propose a spin-insensitive design principle based on metasurfaces that can perform identical functionality (on co- and cross-polarization channels) irrespective of the handedness of incident/transmitted light. As a proof of concept, we design and numerically realize two types of spin-insensitive wavefront engineering devices: (1) spin-insensitive meta-hologram and (2) spin-insensitive beam deflector with power splitting functionality. The proposed work is expected to open up new avenues for developing spin-independent metasurfaces-based devices.

Keywords: metasurface; spin-insensitivity; meta-hologram; beam splitter.
DOI: 10.3788/COL202321.010006

1. Introduction

Metasurfaces, the two-dimensional version of artificially engineered metal/dielectric structures that control the amplitude, phase, and polarization of light by varying the spatial dimensions and orientation of meta-elements, are promising candidates to mold the outgoing wavefront[1–10]. Polarization of the incident light plays a key role in light–matter interaction for wavefront manipulation; however, geometry of meta-elements makes the metasurfaces sensitive to the incident polarization of the light. There have been several efforts to realize single-layered polarization-insensitive metasurfaces for wavefront engineering functionalities, e.g., meta-holograms, metalenses, and beam steering for linear and circular polarization[11–16]. For circularly polarized (CP) wavefront manipulation, these metasurfaces either use propagation phase or compound geometric and propagation phase to obtain the desired phase profiles on CP orthogonal polarization. Polarization-insensitive metasurfaces involving compound phase modulation merge the propagation phase with the polarization-insensitive geometric phase[17–20]. However, such metasurfaces cannot be considered spin-insensitive because they do not undergo any wavefront change for circularly co-polarized light.

For CP wavefront manipulation, the geometric phase can be imposed on the transmitted light independently as well as collectively with the propagation phase for various metasurfaces-based photonic applications[21–32]. In compound phase modulation, the energy in the CP transmitted state as the input cannot be eliminated totally[33]; therefore, researchers have started to explore both co- and cross-polarization states by partially distributing

the output energy[34,35]. By this approach, in a single-layered metasurface, the transmitted phase on three out of four combinations of input and output polarization states can be controlled flexibly for different applications. However, to the best of our knowledge, none of the work has been reported that encodes the same information on all four transmitted polarization states. Here, to realize spin-insensitive functionality through metasurfaces, we use compound phase modulation by merging the propagation phase with the polarization-insensitive geometric phase and utilize both co- and cross-CP channels by partially distributing the energy among them. As a proof of concept, we encode a hologram on the single-layered non-interleaved metasurface, which displays a holographic image for any input and output combination of the CP state. Furthermore, we also numerically realize a spin-free beam deflector, which remains insensitive to the spin of the incident light. The proposed design principle is expected to pave a route to realizing next-generation spin-insensitive integrated photonic systems for communication, imaging, and information processing.

2. Working Principle, Simulation Results, and Discussion

The mathematical description of the desired functionality can be understood through the Jones transmission matrix for the CP input E_{in} and output E^{out} electric field as[33,34,36]

$$J = R(\theta)\begin{bmatrix} e^{i\phi_{\text{RR}}} & e^{i\phi_{\text{RL}}} \\ e^{i\phi_{\text{LR}}} & e^{i\phi_{\text{LL}}} \end{bmatrix} R(-\theta) = \begin{bmatrix} e^{i\phi_{\text{RR}}} & e^{i(\phi_{\text{RL}}\pm 2\sigma\theta+\frac{\pi}{2})} \\ e^{i(\phi_{\text{LR}}\mp 2\sigma\theta+\frac{\pi}{2})} & e^{i\phi_{\text{LL}}} \end{bmatrix}, \tag{1}$$

where $R(\theta)$ is the rotation matrix, and $\pm 2\sigma\theta$ or $\mp 2\sigma\theta$ are geometric phases (rotation-dependent equal and opposite phases for CP orthogonal polarizations), with $\pm\sigma$ or $\mp\sigma$ indicating the handedness of the CP light. Herein, $+\sigma$ and $-\sigma$ denote the right circular polarization (RCP) and the left circular polarization (LCP) light, respectively. ϕ_{RR}, ϕ_{LR}, ϕ_{RL}, and ϕ_{LL} are the propagation phases, which can be tailored through the physical dimensions of the nanobrick, and it can be determined through the phase average of the linearly orthogonal polarizations as $\frac{\phi_{xx}+\phi_{yy}}{2}$. The left/right subscripts represent the output/input CP state and L/R define the LCP/RCP state. For $+\sigma$ incident light, the transmitted electric field can be determined as

$$E^{\text{out}}_{+\sigma} = JE_{\text{in}} = \begin{bmatrix} e^{i\phi_{\text{RR}}} & e^{i(\phi_{\text{RL}}+2\sigma\theta+\frac{\pi}{2})} \\ e^{i(\phi_{\text{LR}}-2\sigma\theta+\frac{\pi}{2})} & e^{i\phi_{\text{LL}}} \end{bmatrix}\begin{bmatrix} 1 \\ 0 \end{bmatrix} = \begin{bmatrix} e^{i\phi_{\text{RR}}} \\ e^{i(\phi_{\text{LR}}-2\sigma\theta+\frac{\pi}{2})} \end{bmatrix}. \tag{2}$$

Similarly, for the $-\sigma$ incident light, the transmitted electric field can be determined as

$$E^{\text{out}}_{-\sigma} = JE_{\text{in}} = \begin{bmatrix} e^{i\phi_{\text{RR}}} & e^{i(\phi_{\text{RL}}+2\sigma\theta+\frac{\pi}{2})} \\ e^{i(\phi_{\text{LR}}-2\sigma\theta+\frac{\pi}{2})} & e^{i\phi_{\text{LL}}} \end{bmatrix}\begin{bmatrix} 0 \\ 1 \end{bmatrix} = \begin{bmatrix} e^{i(\phi_{\text{RL}}+2\sigma\theta+\frac{\pi}{2})} \\ e^{i\phi_{\text{LL}}} \end{bmatrix}. \tag{3}$$

In Eqs. (2) and (3), the terms with propagation phase only can be referred as co-polarization transmission channels, whereas the expression with both propagation and geometric phase can be referred as cross-polarization channels. These expressions indicate that both (co- and cross-) transmission channels can be manipulated through the suitable phase profile selection.

In our work, to design spin-insensitive metasurfaces, the inherent spin-locked geometric phase restriction is lifted up by fixing the rotation angle at "θ=0°" or "θ=90°." In this way, exponential expressions for the geometric phase (cross-polarization channels) provide the same phase profiles, indicating that circular orthogonal polarization channels experience the same phase shift; thus, the geometric phase for these two rotation angles can be considered as polarization-insensitive phase shift. In single-layered metasurfaces, the phase shift in CP co-polarization is always same. It is worth noting that, in order to distribute the energy equally in co- and cross-polarization channels, the phase difference between two linearly orthogonal polarizations should be equal to $\Delta\phi = \phi_{xx} - \phi_{yy} = \pi/2$[34]. If the co- and cross-polarization channels exhibit a phase relationship such that $E^{\text{out}}_{+\sigma} = \begin{bmatrix} \phi_1(\text{Co}) \\ \phi_2 = \phi_1 + \frac{\pi}{2}(\text{Cross}) \end{bmatrix}$ and $E^{\text{out}}_{-\sigma} = \begin{bmatrix} \phi_3 = \phi_1 + \frac{\pi}{2}(\text{Cross}) \\ \phi_4 = \phi_1(\text{Co}) \end{bmatrix}$, then both transmission channels modulate the incoming wavefront in the same way for LCP and RCP light illumination, and the design can be regarded as spin-insensitive. For single-layered non-interleaved metasurfaces, such a kind of phase connection can be conveniently established by fixing the geometric phase value and modulating the propagation phase.

The illustration in Fig. 1(a) presents the unit cell, which consists of silicon nanobricks with the height of $H = 420$ nm placed on the glass substrate. The physical dimensions of the nanobrick in the x and y directions "$L_x = L_y$" determine the propagation phase, and the orientation angle θ between the x axis and local coordinate "u" determines the geometric phase. Here, we obtain the propagation phase by modifying the side dimensions and merging it with fixed geometric phase by rotating the nanobrick at θ=0° or θ=90° depending upon the fast axis [Fig. 1(a)]. Hence, the 2π phase control can be achieved to realize the proposed functionality. It is worth mentioning that the choice of nanobrick instead of isotropic structure facilitates partial distribution of output energy in CP co- and cross-polarization channels. To obtain the 2π phase control, the side dimensions of the nanobrick are swept from 50 to 250 nm at θ=0° by using the finite difference time domain (FDTD) simulation tool (Lumerical) under the normally incident linearly orthogonal polarizations. The wavelength of incident light is $\lambda = 780$ nm. The corresponding numerically simulated amplitude and phase delays are shown in Fig. 1(b). A library search approach is used to pick the nanobricks that satisfy the "$\Delta\phi \approx \pi/2$" phase difference [Fig. 1(c)] between the fast and slow axes, which guarantees

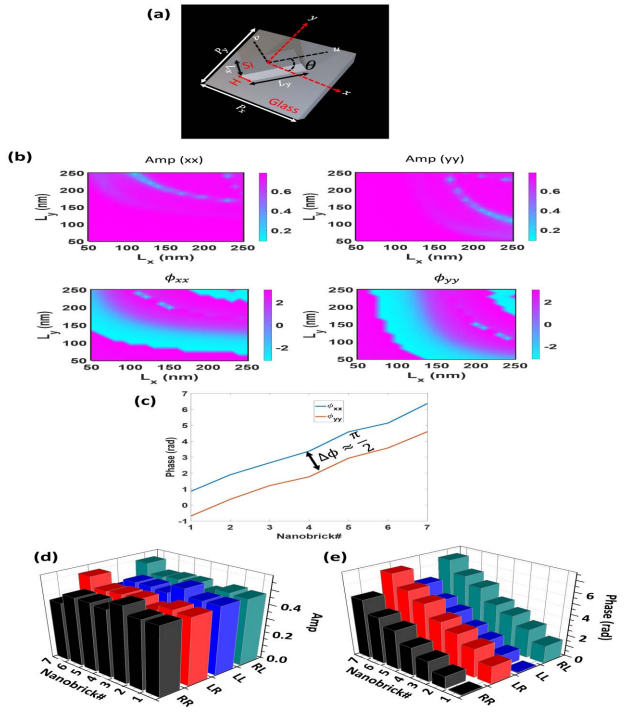

Fig. 1. (a) Unit cell 3D schematic. The period $P_x = P_y$ is set to be 400 nm. (b) Library of amplitude and phase delays (radian) obtained through the parametric scan for linearly orthogonal polarizations. (c)–(e) Numerically simulated results of phase delays and amplitude of optimized nanobricks.

almost equal amplitude distribution in CP co- and cross-transmission channels and fulfills the $0-2\pi$ phase span. The optimized parametric values of nanobricks are presented in Table 1. Figure 1(d) shows that, for RCP/LCP incident light, these basic nanobricks partially distribute the amplitude between the CP co- and cross- [(Amp_RR and Amp_LR) or (Amp_LL and Amp_RL)] transmission channels. The amplitude distribution is the same for CP co-polarization (Amp_RR= Amp_LL) and cross-polarization (Amp_LR = Amp_RL) channels. The optimized nanobricks provide the discrete phase coverage of 2π with a phase interval of $2\pi/7$, as presented in Fig. 1(e). It is shown that the pair of co-polarization channels (RR and LL) has the same profiles, and the pair of cross-polarization channels (LR and RL) experiences the additional $\pi/2$ phase shift. Based on optimized parametric values, in the following, we design and numerically realize two types of spin-insensitive metasurface designs: (1) spin-insensitive meta-hologram and (2) spin-insensitive beam deflector possessing power splitting functionality.

Table 1. Optimized Parametric Values of Basic Nanobricks.

Nanobrick #	1	2	3	4	5	6	7
L_x (nm)	158	174	250	90	215	153	154
L_y (nm)	138	142	138	218	55	110	130

2.1. Spin-insensitive meta-hologram

Holography, the technique of recording and reconstructing wavefronts, has seen the evolution of three-dimensional (3D) displays from its beginnings. Conventional holographic techniques record the interference between the coherent reference beam and target object and reconstruct the virtual 3D image through reference beam illumination[37,38]. In recent years, computer-generated holography (CGH) is replacing conventional techniques by calculating the amplitude and phase information of the target's object through a computer without any complex recording process[39]. In general, CGH techniques use the spatial light modulator (SLM) for encoding and decoding; however, large pixel size limits its functionality to obtain holographic images with high resolution[40,41].

The subwavelength-scaled feature size of meta-elements overcomes the SLM's pixel size limit and opens new frontiers for optical and holographic devices. Metasurface holography can be achieved by precisely mapping the encoding image's configuration (phase and/or amplitude) with the meta-elements at the interface according to their position and local scattering properties. Metasurface holography can be categorized into three major types: phase-only holography, amplitude-only holography, and complex (combined amplitude and phase) holography[42]. To design a metasurface holographic device (phase only or complex), discrete phase shifts are the crucial information that can be tailored by engineering the spatial dimensions and/or orientation of the meta-elements depending upon the input/output polarization of the light. Several polarization-dependent and independent metasurface holograms have been reported for linearly polarized light[11,14,43–47]. For CP light, most meta-holograms involving the spin of light display the holographic image on the cross polarization, making them sensitive to handedness of the incident light[48–52]. In this work, we propose the spin-insensitive metasurface hologram, which displays the identical holographic image irrespective of the spin of incident/output polarization through compound phase modulation by controlling the spatial dimension and orientation of meta-elements.

The schematic of the proposed spin-insensitive metasurfaces hologram is shown in Fig. 2. It is presented that the light at the output with the LCP or RCP state displays an identical holographic image regardless of the spin of incident light. To design the meta-hologram, phase information of the target image with the letters "NRC" [Fig. 3(a)] is extracted through the Gerchberg–Saxton algorithm[53]. The reconstructed hologram is shown in Fig. 3(b). Then, the mapping of the nanobrick's discrete phase levels is performed with the hologram's phase mask, and two-dimensional (2D) matrices containing the physical dimensions of the nanobricks in the spatial domain are obtained. These spatially distributed parametric values of nanobricks are then imported onto the interface of the glass substrate. When the RCP light is normally incident on the metasurface, the spatially distributed nanobricks interact with the incoming light and reproduce the holographic image of the letters "NRC" on both transmitted channels, i.e., "RR and LR." Similarly, by switching

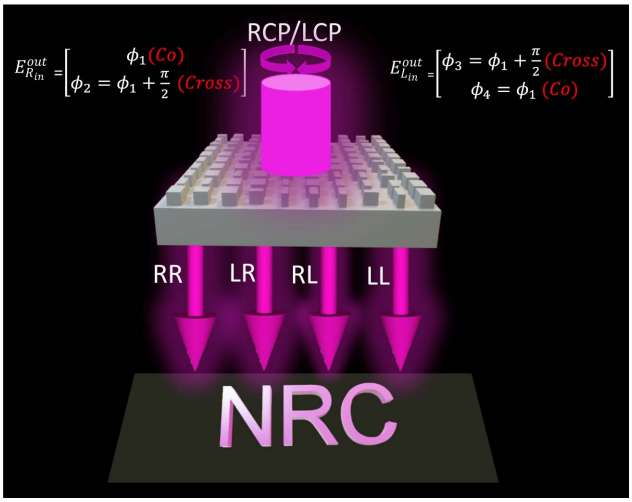

Fig. 2. Schematic illustration of spin-insensitive meta-hologram. The proposed scheme reconstructs the identical image "NRC" regardless of the spin of the incident and transmitted light.

the spin of the incident light to LCP, the spatially distributed nanobricks reproduce the same image on the "RL and LL" channels; the far-field results are shown in Figs. 3(c). The transmission channels "RR" and "LL" reconstruct the same image due to "$\phi_1 = \phi_4$," and, because of the relative additional phase shift "$\pi/2$," the same holographic image appears on the "LR" and "RL" channels.

2.2. Spin-insensitive beam deflector with power splitting functionality

The proposed design principle can also be implied to realize other polarization-insensitive metasurfaces devices. Similar to the meta-hologram, previously reported metasurfaces-based CP beam steering devices (beam deflectors and splitters) only utilize the cross-polarization channels[26,54]. In the following, for RCP/LCP incident light, a spin-insensitive beam deflector possessing the beam splitting functionality in CP orthogonal channels at output is designed. Such beam deflectors can refract

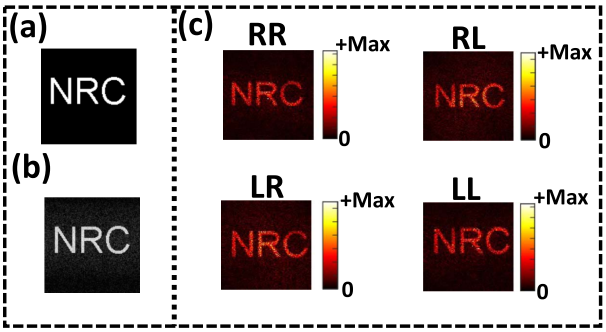

Fig. 3. (a) Target object and (b) reconstructed CGH. (c) Numerically simulated FDTD results of the proposed spin-insensitive meta-hologram. The identical image "NRC" is reconstructed on all four transmitted CP channels.

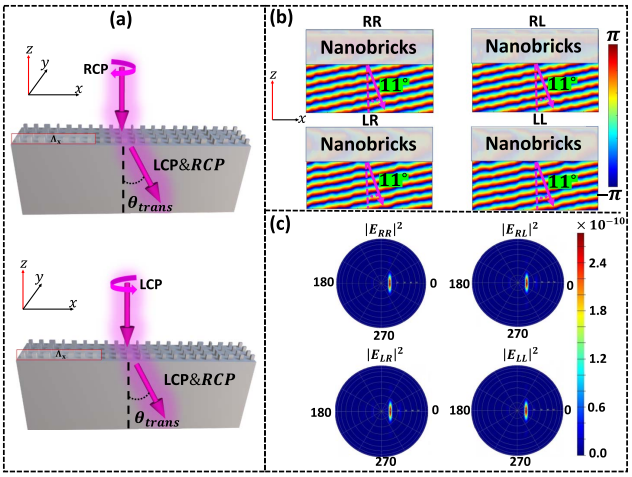

Fig. 4. (a) Schematic of spin-insensitive beam deflector. Numerically simulated results of (b) near-field and (c) far-field under RCP and LCP light.

the transmitted CP orthogonal beams (LCP and RCP) at a specific angle with an energy distribution ratio of 50:50. In order to realize the proposed beam deflector design, the phase function for the normally incident light can be designed as follows: $\mathrm{d}\phi(x,\lambda) = \frac{2\pi}{\lambda} n_t \mathrm{d}x \sin\theta_{\mathrm{trans}}$, in which λ is the operating wavelength, x is the lateral position on the metasurface, n_t is the refractive index of transmission media, and dx is the period size. At operating frequency, the transmission/refraction angle θ_{trans} can be determined through the size of the super cell composed of unit cells covering the $0-2\pi$ discrete phase span.

The schematic of the proposed spin-insensitive beam deflector is shown in Fig. 4(a). It is shown that under CP (LCP/RCP), both co- and cross-polarized lights deflect at θ_{trans}. To numerically realize the proposed functionality, three super cells composed of seven basic nanobricks are distributed in four rows. The size of each super cell in the x direction is $\Lambda_x = 400\,\mathrm{nm} \times 7 = 2800\,\mathrm{nm}$. Hence, the transmission angle in glass ($n_t = 1.46$) can be calculated as $\theta_{\mathrm{trans}} = \arcsin(\frac{780\,\mathrm{nm}\times 2\pi}{2\pi\times 2800\times 1.46\,\mathrm{nm}}) = 10.99°$. The numerically calculated near-field and far-field results are shown in Figs. 4(b) and 4(c), which validate the analytical results and show that both CP co- and cross-polarization beams are deflecting at the same angle. Furthermore, the power of incident CP light is partially splitting in co- and cross-polarization channels (approximately 48% in each channel) under RCP/LCP light. It is worth noting here that the additional relative phase shift "$\pi/2$" does not significantly change the refraction angle and power in CP cross-polarization channels. The proposed meta-hologram and spin-insensitive designs can be experimentally validated through standard electron beam lithography by following the process reported in Refs. [12,55].

3. Conclusion

In summary, we proposed and numerically realized spin-independent metasurfaces for CP transmission channels using compound propagation and polarization-insensitive geometric

phase modulation. By exploring both the co- and cross-transmission channels, the compound propagation and polarization-insensitive geometric phase modulation impose indistinct phase, i.e., $\phi_1 = \phi_4$, on CP co-polarization transmission channels, i.e., "RR" and "LL." Meanwhile, the transmitted light experiences an additional relative phase shift of "$\pi/2$" on the cross-polarization channels, i.e., "LR" and "RL." Such phase distribution can achieve spin-insensitive wavefront engineering functionality for CP outgoing light. This paper incorporates spin-insensitive functionality in meta-hologram and metasurface-based beam deflectors by establishing the desired phase relationships on all CP transmission channels. The numerically simulated results of the meta-hologram reconstruct the same image of the letters "NRC" on all four CP transmission channels regardless of the spin of the incident light. Similarly, the beam deflector design refracts the light at 11° for all four CP transmission channels with equal power distribution (approximately 48% into each co- and cross-transmission channel for RCP/LCP incidence). It is expected that the proposed design principle may pave a route to realizing next-generation spin-insensitive integrated photonic systems for communication, imaging, and information processing.

References

1. N. Yu, P. Genevet, M. A. Kats, F. Aieta, J. P. Tetienne, F. Capasso, and Z. Gaburro, "Light propagation with phase discontinuities: generalized laws of reflection and refraction," Science **334**, 333 (2011).
2. N. Yu and F. Capasso, "Flat optics with designer metasurfaces," Nat. Mater. **13**, 139 (2014).
3. H. Xu, Y. Wang, C. Wang, M. Wang, S. Wang, F. Ding, Y. Huang, X. Zhang, H. Liu, X. Ling, and Wei Huang, "Deterministic approach to achieve full-polarization cloak," Research **2021**, 6382172 (2021).
4. H. Xu, G. Hu, Y. Wang, C. Wang, M. Wang, S. Wang, Y. Huang, P. Genevet, W. Huang, and C. Qiu, "Polarization-insensitive 3D conformal-skin metasurface cloak," Light Sci. Appl. **10**, 75 (2021).
5. H. Xu, L. Han, Y. Li, Y. Sun, J. Zhao, S. Zhang, and C. Qiu, "Completely spin-decoupled dual-phase hybrid metasurfaces for arbitrary wavefront control," ACS Photonics **6**, 211 (2018).
6. H. Zhao, X. Wang, B. Quan, S. Liu, and Y. Zhang, "High-efficiency phase and polarization modulation metasurfaces," Adv. Photon. Res. **3**, 2100199 (2022).
7. R. Xie, D. Zhang, X. Wang, S. An, B. Zheng, H. Zhang, G. Zhai, L. Li, and J. Ding, "Multichannel high-efficiency metasurfaces based on tri-band single-cell meta-atoms with independent complex-amplitude modulations," Adv. Photon. Res. **2**, 2100088 (2021).
8. A. U. R. Khalid, J. Liu, N. Ullah, and S. Jia, "Tunable beam deflection based on plasmonic resonators mounted freestanding thermoresponsive hydrogel," Chin. Opt. Lett. **18**, 062402 (2020).
9. F. Feng, S. Wei, L. Li, C. Min, X. Yuan, and M. Somekh, "Spin-orbit coupling controlled near-field propagation and focusing of Bloch surface wave," Opt. Express **27**, 27536 (2019).
10. F. Feng, G. Si, C. Min, X. Yuan, and M. Somekh, "On-chip plasmonic spin-Hall nanograting for simultaneously detecting phase and polarization singularities," Light Sci. Appl. **9**, 95 (2020).
11. X. Zhang, X. Li, J. Jin, M. Pu, X. Ma, J. Luo, Y. Guo, C. Wang, and X. Luo, "Polarization-independent broadband meta-holograms via polarization-dependent nanoholes," Nanoscale **10**, 9304 (2018).
12. Q.-T. Li, F. Dong, B. Wang, F. Gan, J. Chen, Z. Song, L. Xu, W. Chu, Y.-F. Xiao, Q. Gong, and Y. Li, "Polarization-independent and high-efficiency dielectric metasurfaces for visible light," Opt. Express **24**, 16309 (2016).
13. A. Ozer, N. Yilmaz, H. Kocer, and H. Kurt, "Polarization-insensitive beam splitters using all-dielectric phase gradient metasurfaces at visible wavelengths," Opt. Lett. **43**, 4350 (2018).
14. X. Zhang, D. Tang, L. Zhou, J. Jiao, D. Feng, G. Liang, and Y. Guo, "Polarization-insensitive colorful meta-holography employing anisotropic nanostructures," Nanoscale **11**, 20238 (2019).
15. C. Guan, X. Ding, Z. Wang, K. Zhang, M. Jin, S. N. Burokur, and Q. Wu, "Helicity-switched hologram utilizing a polarization-free multi-bit coding metasurface," Opt. Express **28**, 22669 (2020).
16. W. T. Chen, A. Y. Zhu, V. Sanjeev, M. Khorasaninejad, Z. Shi, E. Lee, and F. Capasso, "A broadband achromatic metalens for focusing and imaging in the visible," Nat. Nanotechnol. **13**, 220 (2018).
17. J. Xu, X. Tian, P. Ding, K. Xu, and Z.-Y. Li, "$Ge_2Sb_2Se_4Te_1$-based multifunctional metalenses for polarization-independent, switchable and dual-mode focusing in the mid-infrared region," Opt. Express **29**, 44227 (2021).
18. Y. Gao, J. Gu, R. Jia, Z. Tian, C. Ouyang, J. Han, and W. Zhang, "Polarization independent achromatic meta-lens designed for the terahertz domain," Front. Phys. **8**, 606693 (2020).
19. X. Zang, W. Xu, M. Gu, B. Yao, L. Chen, Y. Peng, J. Xie, A. V. Balakin, A. P. Shkurinov, Y. Zhu, and S. Zhuang, "Polarization-insensitive metalens with extended focal depth and longitudinal high-tolerance imaging," Adv. Opt. Mater. **8**, 1901342 (2020).
20. T. Sun, J. Hu, S. Ma, F. Xu, and C. Wang, "Polarization-insensitive achromatic metalens based on computational wavefront coding," Opt. Express **29**, 31902 (2021).
21. G. Zheng, H. Mühlenbernd, M. Kenney, G. Li, T. Zentgraf, and S. Zhang, "Metasurface holograms reaching 80% efficiency," Nat. Nanotechnol. **10**, 308 (2015).
22. D. Wen, F. Yue, G. Li, G. Zheng, K. Chan, S. Chen, M. Chen, K. F. Li, P. W. H. Wong, K. W. Cheah, E. Y. B. Pun, S. Zhang, and X. Chen, "Helicity multiplexed broadband metasurface holograms," Nat. Commun. **6**, 8241 (2015).
23. N. Ullah, W. Liu, G. Wang, Z. Wang, A. U. R. Khalid, B. Hu, J. Liu, and Y. Zhang, "Gate-controlled terahertz focusing based on graphene-loaded metasurface," Opt. Express **28**, 2789 (2020).
24. A. U. R. Khalid, F. Feng, N. Ullah, M. Somekh, and X. Yuan, "Exploitation of geometric and propagation phases for spin-dependent rational-multiple complete phase modulation using dielectric metasurfaces," Photonics Res. **10**, 877 (2022).
25. J. Engelberg, C. Zhou, N. Mazurski, J. Bar-David, A. Kristensen, and U. Levy, "Near-IR wide-field-of-view Huygens metalens for outdoor imaging applications," Nanophotonics **9**, 361 (2020).
26. A. U. R. Khalid, F. Feng, M. I. Khan, X. Yuan, and M. G. Somekh, "All-dielectric metasurface designs for spin-tunable beam splitting via simultaneous manipulation of propagation and geometric phases," Opt. Express **30**, 13459 (2022).
27. B. Groever, N. A. Rubin, J. B. Mueller, R. C. Devlin, and F. Capasso, "High-efficiency chiral meta-lens," Sci. Rep. **8**, 7240 (2018).
28. S. Li, X. Li, G. Wang, S. Liu, L. Zhang, C. Zeng, L. Wang, Q. Sun, W. Zhao, and W. Zhang, "Multidimensional manipulation of photonic spin Hall effect with a single-layer dielectric metasurface," Adv. Opt. Mater. **7**, 1801365 (2019).
29. T. Li, X. Xu, B. Fu, S. Wang, B. Li, Z. Wang, and S. Zhu, "Integrating the optical tweezers and spanner onto an individual single-layer metasurface," Photonics Res. **9**, 1062 (2021).
30. Y. Guo, S. Zhang, M. Pu, Q. He, J. Jin, M. Xu, Y. Zhang, P. Gao, and X. Luo, "Spin-decoupled metasurface for simultaneous detection of spin and orbital angular momenta via momentum transformation," Light Sci. Appl. **10**, 63 (2021).
31. J. Chen, F. Zhang, Q. Li, J. Wu, and L. Wu, "A high-efficiency dual-wavelength achromatic metalens based on Pancharatnam–Berry phase manipulation," Opt. Express **26**, 34919 (2018).
32. R. Zhao, B. Sain, Q. Wei, C. Tang, X. Li, T. Weiss, L. Huang, Y. Wang, and T. Zentgraf, "Multichannel vectorial holographic display and encryption," Light Sci. Appl. **7**, 95 (2018).
33. Y. Yuan, S. Sun, Y. Chen, K. Zhang, X. Ding, B. Ratni, Q. Wu, S. N. Burokur, and C.-W. Qiu, "A fully phase-modulated metasurface as an energy-controllable circular polarization router," Adv. Sci. **7**, 2001437 (2020).
34. K. Zhang, Y. Yuan, X. Ding, H. Li, B. Ratni, Q. Wu, J. Liu, S. N. Burokur, and J. Tan, "Polarization-engineered noninterleaved metasurface for integer and

fractional orbital angular momentum multiplexing," Laser Photon. Rev. **15**, 2000351 (2021).
35. C. Zheng, G. Wang, J. Li, J. Li, S. Wang, H. Zhao, M. Li, Z. Yue, Y. Zhang, Y. Zhang, and J. Yao, "All-dielectric metasurface for manipulating the superpositions of orbital angular momentum via spin-decoupling," Adv. Opt. Mater. **9**, 2002007 (2021).
36. C. Chen, S. Gao, X. Xiao, X. Ye, S. Wu, W. Song, H. Li, S. Zhu, and T. Li, "Highly efficient metasurface quarter-wave plate with wave front engineering," Adv. Photon. Res. **2**, 2000154 (2021).
37. D. Gabor, "A new microscopic principle," Nature **161**, 777 (1948).
38. E. N. Leith and J. Upatnieks, "Reconstructed wavefronts and communication theory," J. Opt. Soc. Am. **52**, 1123 (1962).
39. C. Slinger, C. Cameron, and M. Stanley, "Computer-generated holography as a generic display technology," Computer **38**, 46 (2005).
40. X. Li, H. Ren, X. Chen, J. Liu, Q. Li, C. Li, G. Xue, J. Jia, L. Cao, A. Sahu, B. Hu, Y. Wang, G. Jin, and M. Gu, "Athermally photoreduced graphene oxides for three-dimensional holographic images," Nat. Commun. **6**, 6984 (2015).
41. C. Gao, J. Liu, X. Li, G. Xue, J. Jia, and Y. Wang, "Accurate compressed look up table method for CGH in 3D holographic display," Opt. Express **23**, 33194 (2015).
42. L. Huang, S. Zhang, and T. Zentgraf, "Metasurface holography: from fundamentals to applications," Nanophotonics **7**, 1169 (2018).
43. X. Su, G. Li, H. Yang, Z. Zhao, F. Yu, X. Chen, and W. Lu, "A visible high efficiency and polarization-insensitive 34-level dielectric metasurface hologram," RSC Adv. **7**, 26371 (2017).
44. A. U. R. Khalid, J. Liu, Y. Han, N. Ullah, R. Zhao, and Y. Wang, "Multichannel polarization encoded reflective metahologram using VO_2 spacer in visible regime," Opt. Commun. **451**, 211 (2019).
45. C. Guan, J. Liu, X. Ding, Z. Wang, K. Zhang, H. Li, M. Jin, S. N. Burokur, and Q. Wu, "Dual-polarized multiplexed meta-holograms utilizing coding metasurface," Nanophotonics **9**, 3605 (2020).
46. F. Cheng, L. Ding, L. Qiu, D. Nikolov, A. Bauer, J. P. Rolland, and A. N. Vamivakas, "Polarization-switchable holograms based on efficient, broadband multifunctional metasurfaces in the visible regime," Opt. Express **26**, 30678 (2018).
47. A. U. R. Khalid, J. Liu, Y. Han, N. Ullah, S. Jia, and Y. Wang, "Multipurpose thermoresponsive hydrogel: a platform for dynamic holographic display," Opt. Lett. **45**, 479 (2020).
48. M. A. Ansari, I. Kim, I. D. Rukhlenko, M. Zubair, S. Yerci, T. Tauqeer, M. Q. Mehmood, and J. Rho, "Engineering spin and antiferromagnetic resonances to realize an efficient direction-multiplexed visible meta-hologram," Nanoscale Horiz. **5**, 57 (2020).
49. G.-Y. Lee, G. Yoon, S.-Y. Lee, H. Yun, J. Cho, K. Lee, H. Kim, J. Rho, and B. Lee, "Complete amplitude and phase control of light using broadband holographic metasurfaces," Nanoscale **10**, 4237 (2018).
50. J. P. Balthasar Mueller, N. A. Rubin, R. C. Devlin, B. Groever, and F. Capasso, "Metasurface polarization optics: independent phase control of arbitrary orthogonal states of polarization," Phys. Rev. Lett. **118**, 113901 (2017).
51. Q. Jiang, L. Cao, L. Huang, Z. He, and G. Jin, "A complex-amplitude hologram using an ultra-thin dielectric metasurface," Nanoscale **12**, 24162 (2020).
52. F. Qin, Z. Liu, Z. Zhang, Q. Zhang, and J. Xiao, "Broadband full-color multichannel hologram with geometric metasurface," Opt. Express **26**, 11577 (2018).
53. R. W. Gerchberg and W. O. Saxton, "A practical algorithm for the determination of phase from image and diffraction plane pictures," Optik **35**, 237 (1972).
54. L. Huang, X. Chen, H. Muhlenbernd, G. Li, B. Bai, Q. Tan, G. Jin, T. Zentgraf, and S. Zhang, "Dispersionless phase discontinuities for controlling light propagation," Nano Lett. **12**, 5750 (2012).
55. B. Wang, F. Dong, H. Feng, D. Yang, Z. Song, L. Xu, W. Chu, Q. Gong, and Y. Li, "Rochon-prism-like planar circularly polarized beam splitters based on dielectric metasurfaces," ACS Photonics **5**, 1660 (2017).